Eur. Phys. J. A **17**, 457–461 (2003)
DOI 10.1140/epja/i2002-10192-7

THE EUROPEAN PHYSICAL JOURNAL A

Nuclear matter spectral function in the Bethe-Brueckner-Goldstone approach

M. Baldo[a] and L. Lo Monaco

INFN, and Dipartimento di Fisica dell' Università di Catania, via S. Sofia 64, 95123 Catania, Italy

Received: 1 November 2002 /
Published online: 15 July 2003 –

Abstract. The microscopic many-body theory of the Nuclear Equation of State is discussed in the framework of the Bethe-Brueckner-Goldstone method. The expansion is extended up to the three hole-line diagrams contribution. Within the same scheme, the hole spectral function is calculated in nuclear matter to assess the relevance of nucleon-nucleon short-range correlations. The calculation is carried out by using several nucleon-nucleon realistic interactions. Results are compared with other approaches based on variational methods and transport theory. Discrepancies appear in the high-energy region, which is sensitive to short-range correlations, and are due to the different many-body treatment more than to the specific NN interaction used. Both nuclear matter Equation of State and spectral function appear to be dominated by two-body correlations.

PACS. 21.65.+f Nuclear matter – 21.10.Pc Single-particle levels and strength functions

1 Introduction

At the hadron level, the main difficulty in the many-body theory of nuclear matter is the treatment of the strong repulsive core, which dominates the short-range behaviour of the nucleon-nucleon (NN) interaction. One way of overcoming this difficulty is to introduce the two-body scattering G-matrix, which has a much smoother behaviour even for large repulsive core. It is possible to rearrange the perturbation expansion in terms of the reaction G-matrix, in place of the original bare NN interaction, and this procedure is systematically exploited in the Bethe-Brueckner-Goldstone (BBG) expansion [1]. In this work we present the latest results on the nuclear EOS based on BBG expansion. The same approach can be applied to the study of the nucleon spectral function, and we will present some results obtained recently.

2 The BBG expansion and the nuclear EOS

The BBG expansion for the ground-state energy at a given density, *i.e.* the EOS at zero temperature, can be ordered according to the number of independent hole-lines appearing in the diagrams representing the different terms of the expansion. This grouping of diagrams generates the so-called hole-line expansion [2]. The diagrams with a given number n of hole-lines are expected to describe the main contribution to the n-particle correlations in the system. At the two hole-line level of approximation the corresponding summation of the ladder diagrams produces the Brueckner-Hartree-Fock (BHF) approximation, which incorporates the two-particle correlations. The BHF approximation includes the self-consistent procedure of determining the single-particle auxiliary potential, which is an essential ingredient of the method. Once the auxiliary self-consistent potential is introduced, the expansion is implemented by introducing the set of diagrams which include "potential insertions". Formally, the complete summation of the whole diagrammatic series is independent of the particular choice of the auxiliary potential. In practice, if the auxiliary potential is not too exotic, once convergence of the expansion has been reached, the results should be stable under modifications of the single-particle potential. We will use this property as a criterion of convergence.

The summation of the ladder diagrams can be performed by solving the integral equation for the Brueckner G-matrix

$$\begin{aligned}\langle k_1k_2|G(\omega)|k_3k_4\rangle \;=\; &\langle k_1k_2|v|k_3k_4\rangle \;+\; \sum_{k_3'k_4'}\langle k_1k_2|v|k_3'k_4'\rangle \\ &\times\frac{(1-\Theta_{\rm F}(k_3'))\,(1-\Theta_{\rm F}(k_4'))}{\omega-e_{k_3'}-e_{k_4'}} \\ &\times\langle k_3'k_4'|G(\omega)|k_3k_4\rangle\,, \qquad (1)\end{aligned}$$

where $\Theta_{\rm F}(k) = 1$ for $k < k_{\rm F}$ and is zero otherwise, with $k_{\rm F}$ the Fermi momentum. The product $Q(k,k') = (1-\Theta_{\rm F}(k))(1-\Theta_{\rm F}(k'))$, appearing in the kernel of eq. (1),

[a] e-mail: marcello.baldo@ct.infn.it

selects only scattered momenta which lie outside the Fermi sphere, and it is commonly referred to as the "Pauli operator". This G-matrix can be viewed as the in-medium scattering matrix between two nucleons. Indeed, in the BBG expansion the original bare NN interaction is replaced by the G-matrix in all higher-order terms.

The effect of three-body correlations can be calculated by considering the three hole-line diagrams. They can be summed up by introducing a similar generalization of the scattering matrix for three particles. The three-body scattering problem for free particles has received a formal solution by Fadeev [3]. For identical particles the original three integral Fadeev equations reduce to one because of symmetry. The analogous equation and scattering matrix in the case of nuclear matter has been introduced by Bethe [4]. The integral equation, the Bethe-Fadeev equation, reads schematically

$$T^{(3)} = G + G\,X\,\frac{Q_3}{e}\,T^{(3)}, \qquad \text{or}$$
$$\langle k_1k_2k_3|T^{(3)}|k_1'k_2'k_3'\rangle = \langle k_1k_2|G|k_1'k_2'\rangle\delta_K(k_3-k_3')$$
$$+\langle k_1k_2k_3|G_{12}\,X\,\frac{Q_3}{e}\,T^{(3)}|k_1'k_2'k_3'\rangle\,. \qquad (2)$$

The kernel contains the two-body scattering matrix G in place of the bare NN interaction, in line with the BBG scheme. The factor Q_3/e is the analogue of the similar factor appearing in the integral equation for the two-body scattering matrix G, see eq. (1). Therefore, the projection operator Q_3 imposes that all the three-particle states lie above the Fermi energy, and the denominator e is the appropriate energy denominator, namely the energy of the three-particle intermediate state minus the entry energy ω, in close analogy with eq. (1). The real novelty with respect to the two-body case is the operator X. This operator interchanges particle 3 with particle 1 and with particle 2, $X = P_{123} + P_{132}$, where P indicates the operation of cyclic permutation of its indices. The reason for the appearance of the operator X is that no two successive G-matrices can be present in the same pair of particle lines, since the G-matrix already sums up all the two-body ladder processes. Higher-order correlations can be introduced with the help of higher many-body scattering matrix, but we will see that this is not necessary. The results at the BHF level of approximation is reported in fig. 1 in the case of symmetric nuclear matter (solid lines). The two EOS correspond to two different choices of the auxiliary potential, the standard and continuous choices. The former choice set the potential for momenta larger than the Fermi momentum, the latter choice adopts the same Brueckner definition for all momenta. These two choices can be considered as two extreme opposite cases. As one can see, the saturation curves are different for the two prescriptions. However, the apparent discrepancy of 4–5 MeV in the binding energies shown in fig. 1, is about 10% of the calculated potential energy per particle, which is about −40 MeV around saturation. This is the degree of convergence obtained at the Brueckner level. In view of these results it appears mandatory to consider the three hole-line diagrams. The value of their contribution can indeed provide a check of convergence and possibly an accurate EOS. The final EOS obtained by adding the three hole-line contribution is reported in fig. 1, both for the gap choice (squares) and the continuous choice (open circles). Two conclusions can be drawn from these results. i) The two saturation curves in the standard and continuous choices, with the inclusion of the three hole-line diagrams, tend now to collapse in a single EOS. This is a strong indication that a high degree of convergence has been reached. The saturation curves extend from low density to about five times saturation density, and it appears unlikely that the agreement between the two choices is a fortuitous coincidence. ii) The Brueckner EOS within the continuous choice turns out to be already close to the full EOS, *i.e.* in this case the three hole-line contribution is quite small. In first approximation one can adopt the BHF results with the continuous choice as the nuclear matter EOS. Indeed, this is a further indication of convergence. The phenomenological saturation point for symmetric nuclear matter is, however, not reproduced, which confirms the finding in ref. [5]. Usually this drawback is corrected by introducing three-body forces.

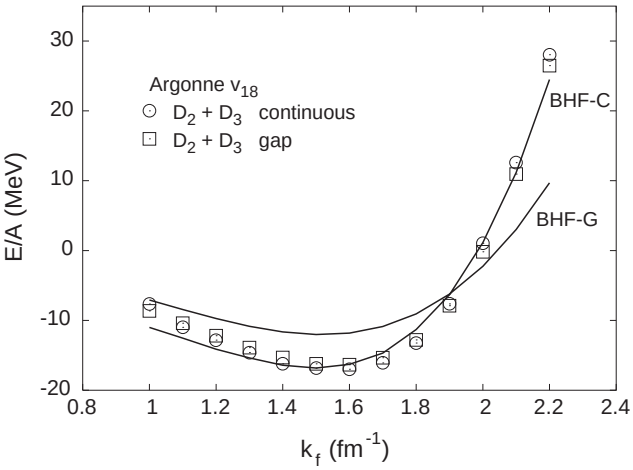

Fig. 1. Nuclear matter saturation curve for the Argonne v_{18} NN potential. The solid lines indicate the results at the Brueckner (two hole-lines) level for the standard (BHF-G) and the continuous choices (BHF-C), respectively. The results obtained adding the three hole-line contribution are given by the open squares (standard choice) and the open circles (continuous choice).

3 Spectral function

In the previous section we saw that a suitable and natural choice of the single-particle potential is able to incorporate a relevant amount of the NN correlations, and consequently two-body correlations dominate the binding energy of nuclear matter. It is not at all obvious that this is still valid for other properties of nuclear matter. In pioneering works by the Bochum group [6] within the so-called e^S method, which is quite similar to the BBG method, it was found that the momentum distribution in

finite nuclei is also dominated by two-body correlations. Another quantity which is expected to be sensitive to nucleon correlations is the single-particle strength function or spectral function. In particular at high momentum and energy transfer the spectral function should be mainly determined by correlations, since for a non-interacting Fermi gas it vanishes in that region. In principle the strength function could be extracted from electron-nucleus scattering data. However, in general only inclusive or semi-inclusive data are available in the region of interest. In this case it is difficult to de-convolute the effects of the final-state interactions and the genuine spectral function cannot be directly extracted from the electron-nucleus cross-sections. Only recently extensive exclusive data [7] are becoming available. The effects of the rescattering on the struck nucleon are still present and must be taken into account before an accurate spectral function can be extracted. Anyhow the results are promising and open quite new possibilities.

In nuclear matter the spectral function corresponding to the nucleon self-energy $M(k,E) = V(k,E) + iW(k,E)$, is given by the well-known result [8]

$$P(k,E) = -\frac{1}{\pi}\mathrm{Im}\,\mathcal{G}(k,E) = \frac{1}{\pi}\frac{W(k,E)}{(-E-\frac{k^2}{2m}-V(k,E))^2+W(k,E)^2}\,, \quad (3)$$

where $\mathcal{G}(k,E)$ is the single-particle Green's function:

$$\mathcal{G}(k,E) = \frac{1}{-E-\frac{k^2}{2m}-V(k,E)-\mathrm{i}W(k,E)}\,. \quad (4)$$

It has to be noticed that the real, $V(k,E)$, and imaginary parts $W(k,E)$ of the self-energy are highly off-shell in the considered energy and momentum ranges. We are interested in the region where E is much greater than the Fermi energy E_F. For high k and E, one finds

$$E+\frac{k^2}{2m} \gg |V(k,E)|, |W(k,E)|\,, \quad (5)$$

as can be seen from the results shown in ref. [9], and the spectral function can thus be approximated with

$$P(k,E) \approx \frac{1}{\pi}\frac{W(k,E)}{\left(E+\frac{k^2}{2m}\right)^2}\,. \quad (6)$$

In the BBG expansion, the whole set of two-hole line contributions to the imaginary part of the nucleon self-energy, in the considered energy range, is summed up by the diagram containing two G-matrices and one-particle–two-hole lines in the intermediate states [9]. The diagram takes into account the presence in the ground state of two-particle two-hole correlations. We will first restrict the analysis to this diagram. We get therefore for $W(k,E)$

$$W(k,E) = \tfrac{1}{2}\sum_{hh'p}\mathrm{Im}\frac{|\langle kp|G\left(e(h)+e(h')\right)|hh'\rangle_a|^2}{E-e(p)+e(h)+e(h')-\mathrm{i}\eta} = \frac{\pi}{2}\sum_{hh'p}|\langle kp|G|hh'\rangle_a|^2\,\delta(-E+e(p)-e(h)-e(h'))\,, \quad (7)$$

where $e(p)$ denotes the self-consistent single-particle energy, the label a means antisymmetrization, and the sum is restricted to states h and h' with a momentum smaller than k_F and p with momentum larger than k_F. Substituting this expression in eq. (6) we get

$$P(k,E) = \tfrac{1}{2}\sum_{hh'p}\frac{|\langle kp|G\left(e(h)+e(h')\right)|hh'\rangle_a|^2}{\left(E+\frac{k^2}{2m}\right)^2} \times \delta\left(E-e(p)+e(h)+e(h')\right)\,. \quad (8)$$

In ref. [10] it has been shown that in the regime of high momentum and energy transfer the strength function of eq. (8) can be cast in a "convolution" form

$$P(k,E) = \frac{\pi^2\rho^2}{16}\int\frac{\mathrm{d}^3P}{(2\pi)^3}\,n_\mathrm{rel}\Big(\big|\mathbf{k}-\tfrac{1}{2}\mathbf{P}\big|\Big)n_\mathrm{cm}^\mathrm{FG}(P) \times \delta\left(E-E_\mathrm{thr}^{(2)}-E^*-e(p)\right)\,. \quad (9)$$

In eq. (9) the quantity E^* is an average excitation energy of the residual system, assumed to be much smaller than the total energy E, calculated with respect to the minimal threshold energy $E_\mathrm{thr}^{(2)}$. The function $n_\mathrm{cm}^\mathrm{FG}$ is the center-of-mass momentum distribution of two particles in a free Fermi gas, and n_rel is the relative momentum distribution of two nucleons in the correlated ground state. The latter, in the considered kinematical region, is proportional to the square of the "defect function" $|\xi(|\mathbf{k}-\frac{1}{2}\mathbf{P}|)|^2$, which is related to the G-matrix according to

$$|\xi\rangle = \frac{Q}{\omega-H_0}G|\phi\rangle\,, \quad (10)$$

where $|\phi\rangle$ is the free two-particle state and H_0 is the one-body part of the nuclear Hamiltonian (including the auxiliary potential). The defect function is a measure of the deviation of the two-body wave function from the free one and therefore it embodies the two-body correlations. The strength function is then directly related to the defect function and to the corresponding correlations.

The physical meaning of eq. (9) is quite transparent. The struck nucleon has a correlated partner with opposite momentum and the correlated pair is moving almost freely inside the nuclear medium. In the work of ref. [10] a convolution formula was indeed used to analyze the spectral function and it was proven to be able of reproducing the results of advanced many-body calculations. In ref. [11] it was shown that the BBG calculations can be accurately approximated by eq. (9), at least for momenta larger than 3 fm^{-1}. The result of eq. (9) not only justifies the convolution formula, but also gives the correct normalization.

An overall view of the strength function, calculated with the complete expression of eq. (3), can be seen in fig. 2. We performed [12] calculations of the nuclear matter spectral function with three different two-body potentials, the Urbana v_{14} [13], the Argonne v_{14} [14] and the Argonne v_{18} [15]. Three-body forces were added, according to the Urbana IX model [16], and adjusted to reproduce the correct saturation point. We checked that the effect of the three-body force on the spectral function is negligible.

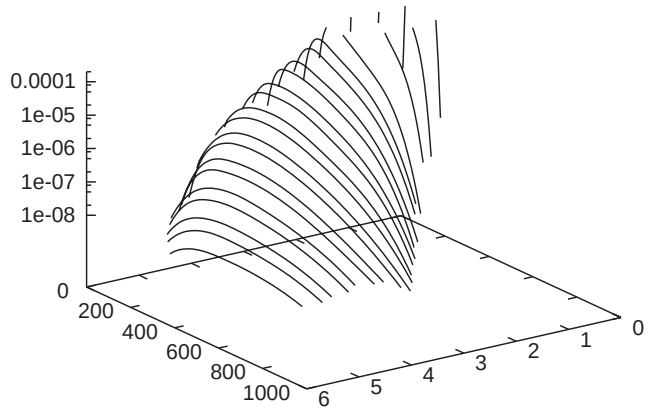

Fig. 2. Three-dimensional view of the nuclear matter strength function $P(k, E)$ (in MeV^{-1}) as a function of momentum k (fm^{-1}) and energy E (MeV). The plot is cut at 10^{-4} to emphasize the energy tail where correlations dominate. The v_{14} NN potential was used. For more details, see the text.

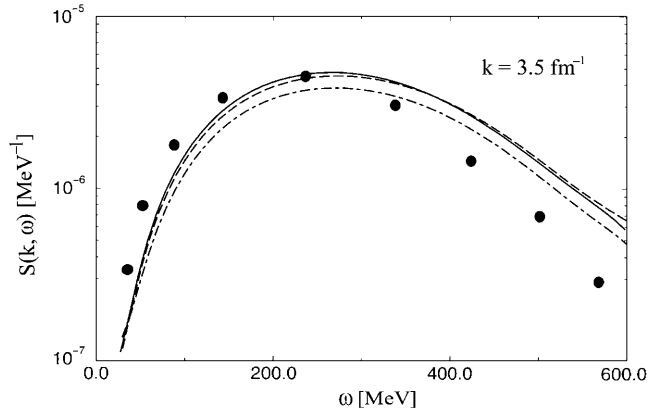

Fig. 3. BBG calculations of the nuclear matter strength function $S(k, \omega)$ as a function of the energy ω for a fixed value of the momentum k. The solid line is the result with the Argonne v_{18} potential, the long-dashed line is obtained with Argonne v_{14} and the dot-dashed line with the Urbana v_{14}. The black dots are the variational results of Benhar *et al.* [17]. The momentum is fixed at $k = 3.5$ fm^{-1}.

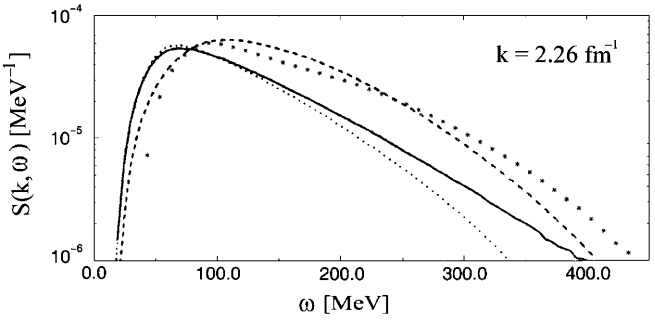

Fig. 4. BBG calculations of the nuclear matter strength function $S(k, \omega)$ as a function of the energy ω for a fixed value of the momentum k. Comparison is made with those of Lehr *et al.*, ref. [18]. The dotted curves are obtained in that work after the first iteration step, the solid curves are their fully self-consistent calculation; the dashed curves show the variational results of Benhar *et al.*, ref. [17]. Our BBG results calculated with the Urbana potential are shown here as asterisks. The momentum is fixed at $k = 2.26$ fm^{-1}.

The scale of the plot is adjusted to emphasize the tail at large energy transfer, where NN correlations dominate. The quasi-particle peak, near the Fermi momentum, is therefore out of the plot (in nuclear matter the strength function diverges at the Fermi surface). One can recognize at large momentum the quasi-elastic peak as a function of energy, where the strength is concentrated and this is a direct consequence of the two-body character of the correlations. For a more quantitative analysis it is more convenient to perform equal momentum cuts. In fig. 3 is shown the spectral function calculated at the the momentum $k = 3.5$ fm^{-1}. The three lines indicate our BBG calculations with different potentials as described in the figure, while the full circles label the variational results of ref. [17], where the Urbana v_{14} was used. For this momentum the dependence on the nucleon-nucleon potential appears quite weak, only in some cases a discrepancy is present, which however does not exceed 20%. Larger deviations in the high-energy region occur between the BBG results and those of ref. [18]. We can conclude that these discrepancies in the high-energy region are due to the many-body treatment and not to the interaction employed.

Similar results are obtained for other values of the momentum k. However, as the k value increases, the discrepancy in the energy tail tends to decrease [12]. It has to be stressed that the overall trend of the spectral function is very similar in the two many-body theories, namely the variational and the BBG schemes, and the absolute values at the maximum are in excellent agreement, without any adjustment of the normalization.

In fig. 4 we compare our results (for the Urbana v_{14} potential) to the fully self-consistent calculation of Lehr *et al.* [18], where the spectral function is calculated within an approximation developed in transport theory. In this case the comparison can be more transparent. The main difference is the inclusion in ref. [18] of the single-particle strength functions in the phase space integral of eq. (7), which implies a self-consistent calculation. Furthermore, in that work the square of the in-medium scattering matrix is approximated by a constant average value, which simplifies the calculation considerably. The average scattering matrix is then adjusted in order to reproduce at best the results of ref. [11]. Therefore, the first-order calculations of ref. [18], indicated by the dotted lines in the figures, are exactly equivalent to our calculations if the G-matrix in eq. (7) is replaced by a constant average value independent of momenta, directly related to the in-medium nucleon-nucleon cross-section [18]. The discrepancy with the BBG calculations is, in this case, only due to this approximation, *i.e.* to the neglect of the G-matrix momentum dependence. This shows the relevance of the momentum-dependent correlations for the determination of the single-particle spectral function. The fact that the introduction of self-consistency moves the high-energy tail towards the BBG behaviour appears misleading, since in

the BBG calculations no self-consistency has been used. This observation seems equally well applicable to the comparison with the variational calculations [17], where also no self-consistency procedure is included in the many-body scheme.

Of course these conclusions do not imply that the self-consistent procedure is not relevant, but only that it must be carried out with the full momentum dependence of the G-matrix. Similar results are obtained for other values of the momentum k, and again the discrepancy tends to decrease as the momentum increases.

4 Conclusions

The calculation of the Nuclear Equation of State in the Bethe-Brueckner-Goldstone expansion indicates that nuclear matter is dominated by two-body correlations up to densities a few times larger than the saturation one. Within the same scheme, the single-particle spectral function was calculated at the two hole-line level of approximation and compared with the results of other many-body theories. In particular, the BBG spectral function appears in fair agreement with the variational method of ref. [17], where higher-order correlations are also included. Some discrepancies in the high-energy tail appear, which however tend to disappear at increasing momentum. These findings, which are independent of the particular NN interaction employed, seem to indicate that also the spectral function is dominated by two-body correlations. The result is consistent with previous calculations of the momentum distribution in finite nuclei in ref. [6].

The comparison of the spectral function with the inclusive data on inelastic electron scattering cannot be direct, since effects of the final-state interactions can be large and dominate in the energy region well below the quasi-elastic peak, where the effect of correlations should be more pronounced. Unfortunately, the inclusion of the final-state interactions requires the calculation of the particle spectral function, and therefore the knowledge of the off-shell in-medium inelastic cross-section. This is a difficult task and up to now an unsolved problem.

Recent exclusive data [7] are more promising. On the one hand, it is possible to separate the inelastic part (*e.g.* the Delta excitation contribution), on the other hand, the comparison is more direct, even if the rescattering in the final states must be taken into account before extracting the nuclear spectral function.

In conclusion, within the BBG scheme a consistent picture of nuclear matter bulk properties and single-particle structure emerges, in which two-body correlations dominate. The extension of these results to finite nuclei will allow a closer comparison with the recent data on exclusive inelastic electron scattering data.

References

1. For a pedagogical introduction, see *Nuclear Methods and the Nuclear Equation of State, Int. Rev. Nucl. Phys.*, edited by M. Baldo, Vol. **8** (World Scientific, Singapore, 1999).
2. B.D. Day, *Brueckner-Bethe calculations of nuclear matter*, in *Proceedings of the International School of Physics "Enrico Fermi", Course LXXIXV*, edited by A. Molinari,, (Editrice Compositori, Bologna, 1983) pp. 1-72; Rev. Mod. Phys. **39**, 719 (1967).
3. L.D. Fadeev, *Mathematical Aspects of the Three-Body Problem in Quantum Scattering Theory* (Davey, New York, 1965).
4. R. Rajaraman, H. Bethe, Rev. Mod. Phys. **39**, 745 (1967).
5. B.D. Day, Phys. Rev. C **24**, 1203 (1981); Phys. Rev. Lett. **47**, 226 (1981).
6. J.G. Zabolitzky, W. Ey, Phys. Lett. B **76**, 527 (1978).
7. D. Rhoe, this issue, p. 439.
8. C. Mahaux, R. Sartor, Phys. Rep. **211**, 53 (1992).
9. M. Baldo, I. Bombaci, G. Giansiracusa, U. Lombardo, C. Mahaux, R. Sartor, Nucl. Phys. A **545**, 741 (1992).
10. M. Baldo, M. Borromeo, C. Ciofi degli Atti, Nucl. Phys. A **604**, 429 (1996).
11. C. Ciofi degli Atti, S. Simula, L.L. Franfurkt, M.I. Strikman, Phys. Rev. C **44**, R7 (1991); C. Ciofi degli Atti, S. Simula, Phys. Rev. C **53**, 1689 (1996).
12. M. Baldo, L. Lo Monaco, Phys. Lett. B **525**, 261 (2002).
13. I.E. Lagaris, V.R. Pandharipande, Nucl. Phys. A **359**, 331 (1981).
14. R.B. Wiringa, R.A. Smith, T.L. Ainsworth, Phys. Rev. C **29**, 1207 (1984).
15. R.B. Wiringa, V.G.J. Stocks, R. Schiavilla, Phys. Rev. **51C**, 38 (1995).
16. R.B. Wiringa, V. Ficks, A. Fabrocini, Phys. Rev. C **38**, 1010 (1988).
17. O. Benhar, A. Fabrocini, S. Fantoni, Nucl. Phys. A **550**, 201 (1992).
18. J. Lehr, M. Effenberger, H. Lenske, S. Leupold, U. Mosel, Phys. Lett. B **483**, 324 (2000).